Late Permian Coals

Subjects: Geology

Contributor: Shifeng Dai

This study reports the mineralogy and geochemistry of the Late Permian C1 Coal from Bole and Laibin mines in eastern Yunnan, Southwestern China (C1 Coal in Laibin mine is composed of three layers termed B1, B2, and B3). The coals are characterized by medium-high ash yields and very low sulfur contents. Compared with average values of trace element concentrations in hard coals worldwide, the Bole and Laibin coals are enriched in V, Co, Cu, Zn, and Se, which were mainly derived from the sediment-source region of the Kangdian Upland. Major minerals in the coal samples and roof and floor strata include quartz, interstratified berthierine/chamosite (B/C), as well as kaolinite, mixed layer illite/smectite, calcite, pyrite, and anatase. Unlike a pure chamosite, the 7 Å peak of interstratified B/C is sharp and narrow, while the 14 Å peak is broad and weak, or absent in some coal samples. Interstratified B/C was largely precipitated from low-temperature Fe-rich and Mg-rich hydrothermal fluids or, in some cases, is an alteration product of kaolinite. Secondary phases of quartz, calcite, pyrite, kaolinite, chalcopyrite, gypsum, and REE-phosphates in the coal samples are the dominant authigenic minerals formed at syngenetic and early diagenetic stages. Four intra-seam partings in C1 Coal, B1, and B3 layers are identified as tonsteins derived from felsic volcanic ashes. These tonsteins consist mainly of cryptocrystalline kaolinite with graupen and vermicular textures, and minor amounts of high-temperature quartz, zircon, apatite, monazite, and anatase. The floor of the C1 Coal in the Bole mine is a tuffaceous claystone and consists of altered high-Ti basalt volcaniclastics, characterized by high concentrations of Zr, Nb, V, Co, Cu, and Zn, low Al_2O_3/TiO_2 ratio (~4.62), high Ti/Y ratio (~900), enrichment of middle rare earth elements, and positive Eu anomalies.

Late Permian coals | minerals in coal | elements in coal | interstratified berthierine/chamosite | tonsteins | Eastern Yunnan

1. Introduction

As with the organic matter in coal, mineral matter is also an important component that significantly influences coal quality [1][2][3]. The abundance, modes of occurrence, and assemblage of mineral matter in coal can provide useful information not only on the conditions of peat deposition, subsequent diagenetic and epigenetic processes, and the regional tectonic history [4][5], but also on assessing the environmental and health impacts of coal processing and utilization [6][7][8][9].

Mineral matter in coal is formed by a range of different processes [2][10], including detrital input from the sediment source region [11][12][13], accumulation of biogenic components [14], precipitation from solutions [15], deposition of volcanic ashes [16][17], and diagenetic and epigenetic alteration. The former two processes are universal in coal

deposits worldwide, while volcanic-influenced coals and intra-seam partings of volcanic origin (i.e., tonstein) have also been observed in many coal deposits [10][18]. The altered volcanic ash layers have been used in some areas as stratigraphic markers or for radiometric age determination if suitable primary minerals (such as sanidine, zircon, and monazite) are present. The mineral matter in altered volcanic ashes can also be used to explain the geologic history and mass extinction events [10][19]. Practically, volcanic ashes in coal may lower the quality of the coal but alkali volcanic ashes may be the cause of significantly enriched critical elements such as Nb, Ta, Zr, Hf, Y, and rare earth elements in coal [10][20][21].

The Late Permian coals from Eastern Yunnan, Southwestern China, have attracted much attention not only because they contain useful records of contemporaneous volcanism during peat deposition and the evolution of the Emeishan mantle plume [12][20][21][22][23][24][25], but also the mineral matter concentrated in the coals (e.g., nano-quartz [26][27] or Fe-rich aluminosilicates [28] in coal in Xuanwei), which is released during coal indoor combustion, leading to the highest female lung cancer mortality rate in the world [26][27][28]. Nanoquartz in the Xuanwei coals was once considered the carcinogen responsible for the high lung cancer rates in the area [26][27]. Although some studies have already found abundant Fe-rich aluminosilicates (e.g., chamosite) in the coals from Xuanwei and adjacent areas [27][29][30], it has just been recognized that chamosite is the newly suspected carcinogen, which plays a significant role in the carcinogenesis pathway by activating inflammatory reactions [28]. There are a number of coal seams in this area. However, not all coals but just C1 Coal is considered the source responsible for lung cancer [27]. It is interesting that abundant Fe-rich aluminosilicate, i.e., interstratified berthierine/chamosite (B/C), was identified in this coal seam in this study but has rarely been previously reported elsewhere [3]. However, it is a common mineral in modern sediments and sedimentary rocks, particularly ironstones [31][32][33][34][35]. Additionally, chlorite is present in coals with different forms such as chamosite $[Fe^{2+}{}_6(Fe^{2+}{}_4,Al_2)[Si_6,Al_2)O_{20}](OH)_{16}]$, cookeite $[Al_4(Li_2,Al_4)[Si_6,Al_2)O_{20}](OH)_{16}]$, pennantite $[Mn^{2+}{}_6(Mn^{2+}{}_4,Al_2)[Si_6,Al_2)O_{20}](OH)_{16}]$, and clinochlore $[Mg_5Al(AlSi_3O_{10})(OH)_8]$ [3]. Different forms of chlorite in coal not only have various chemical compositions but also have formed under different conditions in various stages of coal formation. Precise identification of different forms of chlorite is critical to understand the sources of minerals in coal and the geological processes to which coal has been subjected, and, more importantly, to help with identifying the source responsible for the lung cancer. Therefore, the purpose of this study is to investigate the mineral matter in the C1 Coal and in associated altered volcanic ash layers (including four tonsteins and one floor stratum) from the Bole and Laibin mines (eastern Yunnan, Southwestern China), with special emphasis focusing on the high B/C content in the coal samples.

2. Discussion

2.1. Input of Altered Volcanic Ashes in the Coal-Bearing Strata

Volcanogenic claystones in the coal seams are referred to as tonsteins, bentonites, or K-bentonites, respectively, when kaolinite, smectite, or mixed-layer I/S exceed 50% of the clay mineral assemblages, respectively [18][36]. Southwest China is one of the areas of the world with the most frequent and largest eruptions of volcanic ash during the Late Permian [22][37]. The Late Permian tonsteins, including as many as 30–60 layers in the Xuanwei and

Longtan formations, are widely distributed over areas up to 67,000 km^2 in Western Guizhou and Eastern Yunnan provinces of Southwestern China [38].

The C1 (B1, B2, and B3) coal seam of this study from both the Bole and Laibin mines contains four partings, all of which have been derived from felsic volcanic ash and, therefore, are identified as tonsteins based on the following evidence.

- (1) The partings are all thin (5–6 cm) but laterally continuous throughout the Laibin and Bole coal mines and have a sharp contact with the enclosing coal seam, in which both have general macroscopic characteristics of tonsteins [17][18].

- (2) Due to the high proportions of kaolinite (>50%) and its mode of occurrence, the partings are referred to as tonsteins rather than K-bentonites even though sample B1-3p contains a high proportion of mixed layer I/S. The sample B3-5p can be further classified as a Graupen-tonstein due to the spheroidal aggregates of fine-grained kaolinite (Figure 1D,E). Kaolinite found as vermicular (Figure 1A,E) or tabular (Figure 1C) shape may be formed by alteration of volcanic glass. The vermicular kaolinite is generally considered as evidence for a volcanic origin of claystone within coal seams [12][18][39][40][41]. In addition, the kaolinite-chlorite pseudomorphs after biotite resulted from alteration in the peat swamp [10][18][42].

- (3) High-temperature quartz in the form of angular grains (Figure 2A–C) and corroded quartz crystals with jagged edges or cavities (Figure 1B and Figure 2D) are direct evidence for its derivation from felsic or felsic-intermediate volcanic ashes [12][17]. Angular grains of quartz (Figure 2A) may also be considered as magmatic in origin [38].

- (4) Anatase is generally considered a secondary mineral in tonsteins and is likely derived from the break-down of volcanic ash material [40][43][44]. Anatase crystals with embayments or replacing volcanic glasses (Figure 3A–C) appear to represent alteration products of Ti-rich volcanic glass.

- (5) A small proportion of zircon, apatite, and monazite have been identified in the partings under the SEM. Their preserved subhedral to euhedral crystals (Figure 1G, Figure 3A,F, and Figure 4A–D) are indicative of volcanic input [10][17][42][45][46]. Monazite, if observed in tonsteins, is usually igneous in origin and generally derived from felsic volcanic ashes [10].

- (6) The concentrations of Sc, Ti, V, Cr, Co, Ni, Cu, and Zn are not enriched in the studied partings but are generally elevated in the Late Permian coals of Southwestern China and their roof and floor strata. This indicates that these elements in the four partings have a different (volcanic) origin and have not resulted from erosion of the Kangdian Upland, which is the major sediment source for most of the Late Permian coals in the region [47].

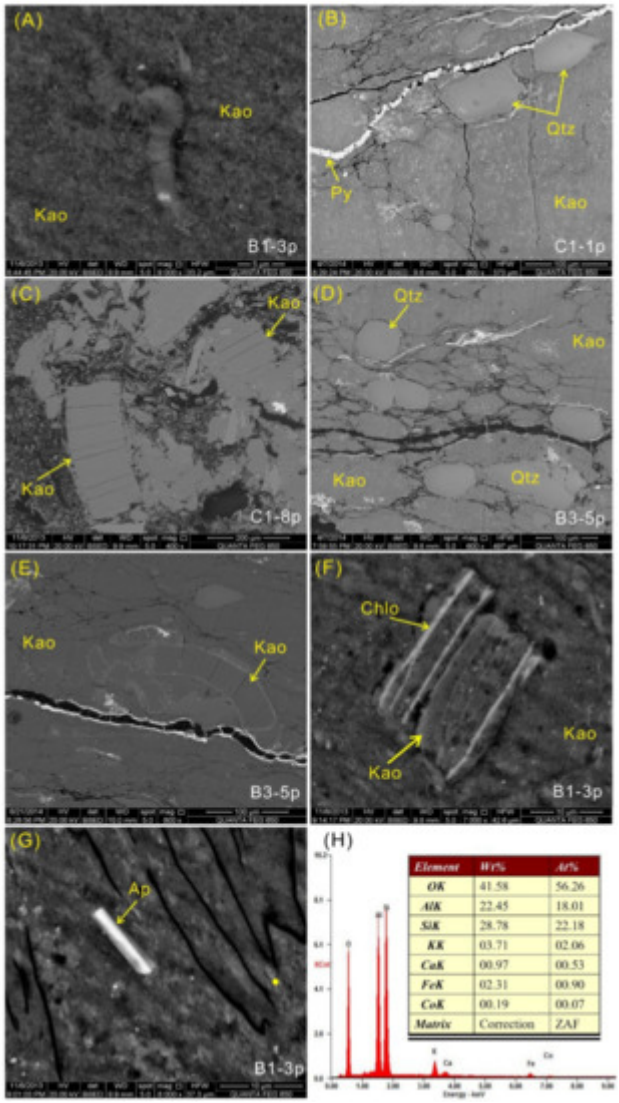

Figure 1. SEM back-scattered electron images of clay minerals in tonsteins and EDS data of selected point. (**A**) Vermicular kaolinite in sample B1-3p. (**B**) Cryptocrystalline kaolinite with quartz and pyrite in sample C1-1t. (**C**) Tabular kaolinite in sample C1-8p, possibly a pseudomorph after biotite or muscovite. (**D**) Elongated pellets and quartz in sample B3-5p. (**E**) Graupen and vermicular kaolinite in sample B3-5p. (**F**) Chlorite intergrown with kaolinite in sample B1-3p. (**G**) Mixed layer I/S and apatite in sample B1-3p. (**H**) EDS spectrum of point in (**G**). Kao: kaolinite. Qtz: quartz. Py: pyrite. Ap: apatite.

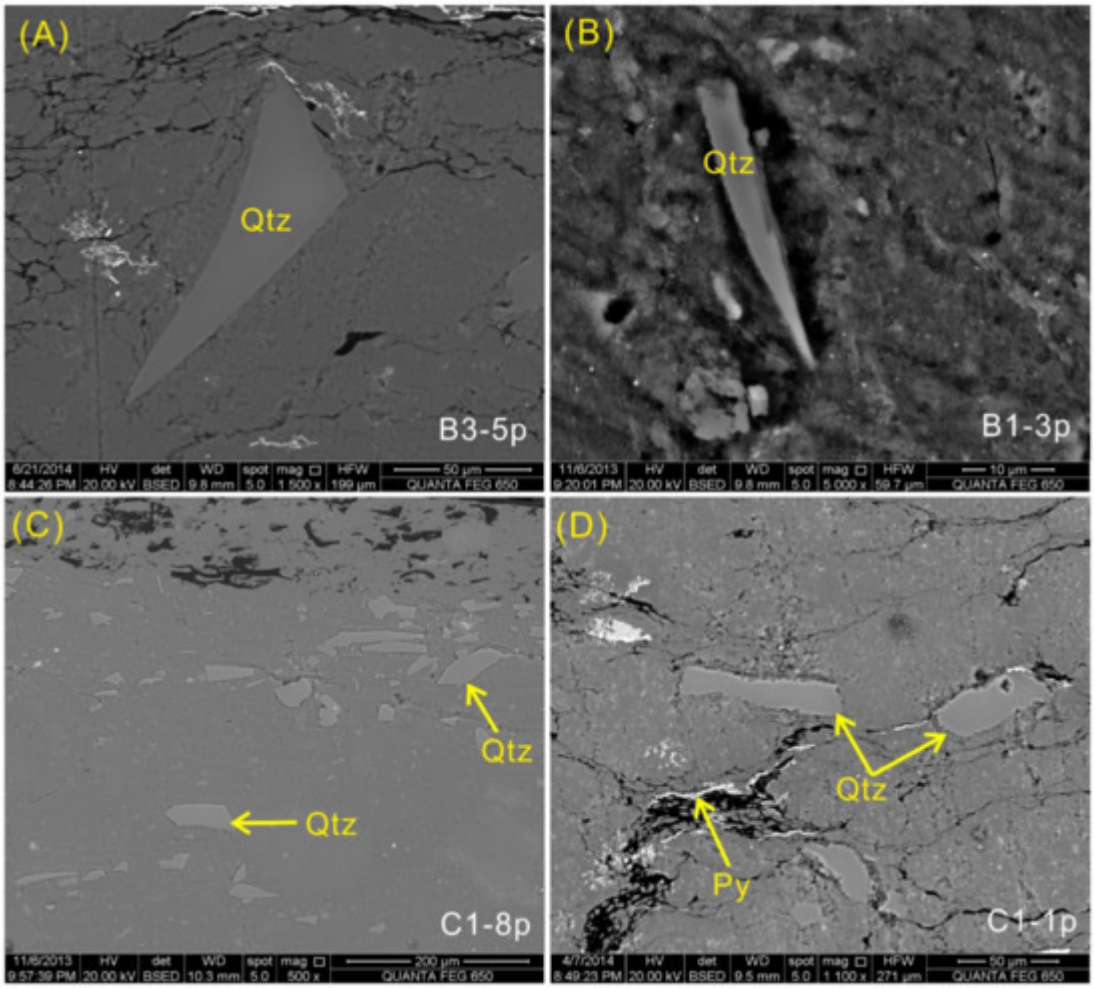

Figure 2. SEM back-scattered electron images of quartz in tonsteins. (**A**–**C**) Sharp-edged quartz in samples B3-5p, B1-3p, and C1-8p. (**D**) Corroded quartz and pyrite veinlets in C1-1t. Qtz: quartz. Py: pyrite.

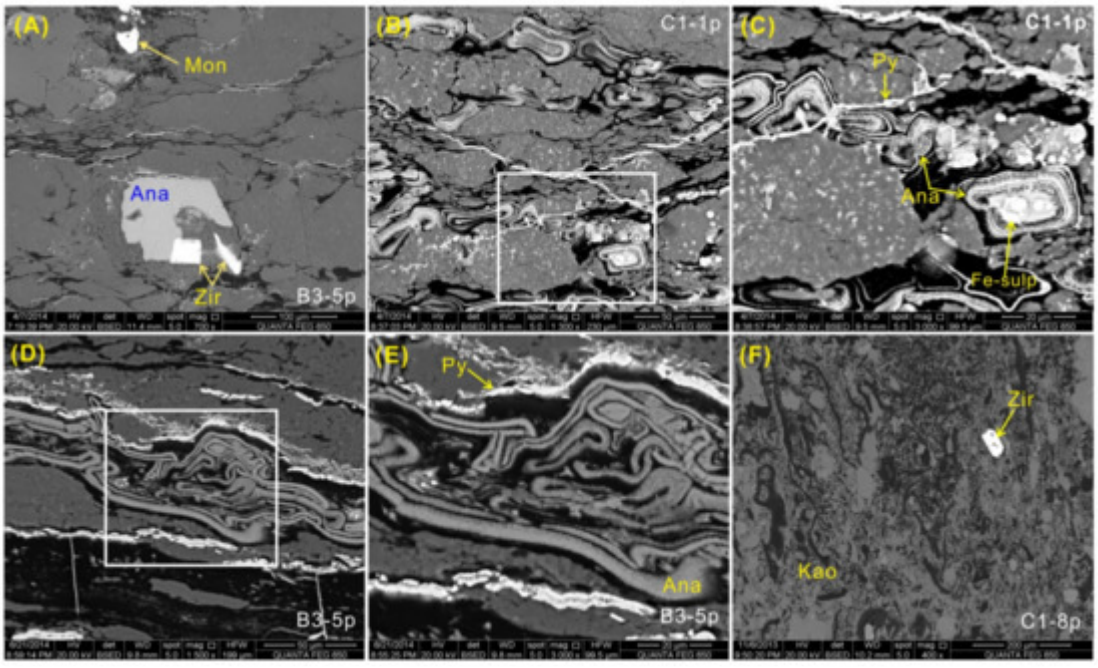

Figure 3. SEM back-scattered electron images of accessory minerals in tonsteins. (**A**) Anatase, zircon, and monazite in B3-5p. (**B**) Anatase possibly replacing glass spherules in C1-1t. (**D**) Fracture-filling anatase and pyrite in B3-5p. (**C**,**E**) are the enlargement of rectangles in (**B**,**D**). (**F**) Zircon in C1-8p. Mon: monazite. Ana: anatase. Zir: zircon. Fe-sulp: Fe-bearing sulfate mineral. Py: pyrite. Kao: kaolinite.

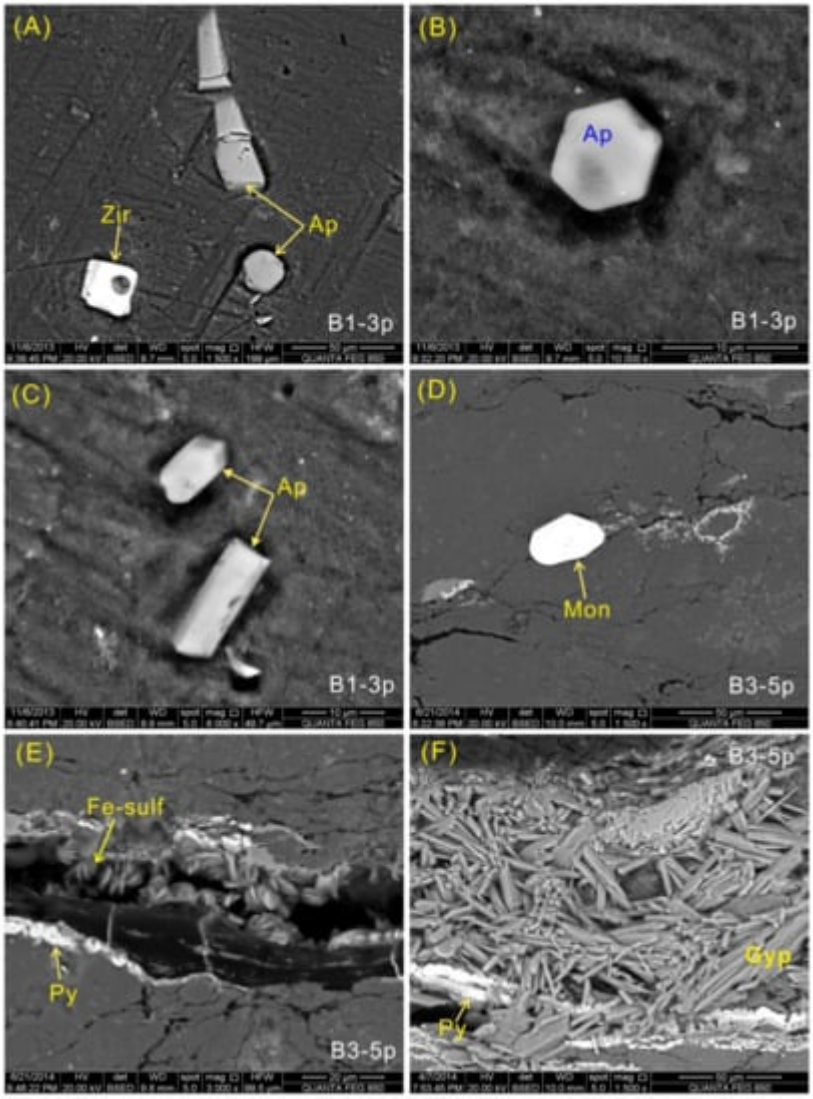

Figure 4. SEM back-scattered electron images of minerals in tonsteins. (**A**) Apatite and zircon in B1-3p. (**B**,**C**) Apatite crystals disseminated in the kaolinite matrix in B1-3p. (**D**) Monazite in B3-5p. (**E**) Fracture-filling pyrite and iron-sulfate mineral in B3-5p. (**F**) Euhedral gypsum in B3-5p. Zir: zircon. Ap: apatite. Mon: monazite. Py: pyrite. Gyp: gypsum.

The Al_2O_3/TiO_2 ratio is relatively stable during surficial weathering, hydrothermal alteration, and volcanic processes [48][49][50] and, therefore, it can be used as a useful provenance indicator for sedimentary rocks (including coal), and for classification of altered volcanic ash [10][51]. Typical Al_2O_3/TiO_2 ratios for sediments or tonsteins derived from mafic, intermediate, and felsic igneous rocks are 3–8, 8–21, and 21–70, respectively [10][51]. The Al_2O_3/TiO_2 ratios of the four studied partings range from 54.8 to 179 (Figure 5), which, along with the distinct negative Eu anomaly of

the REY distribution patterns (Figure 6A), indicates a felsic origin. These tonsteins may be correlated with other Upper Permian volcaniclastic rocks of South China, for which their origin is still uncertain [52][53][54].

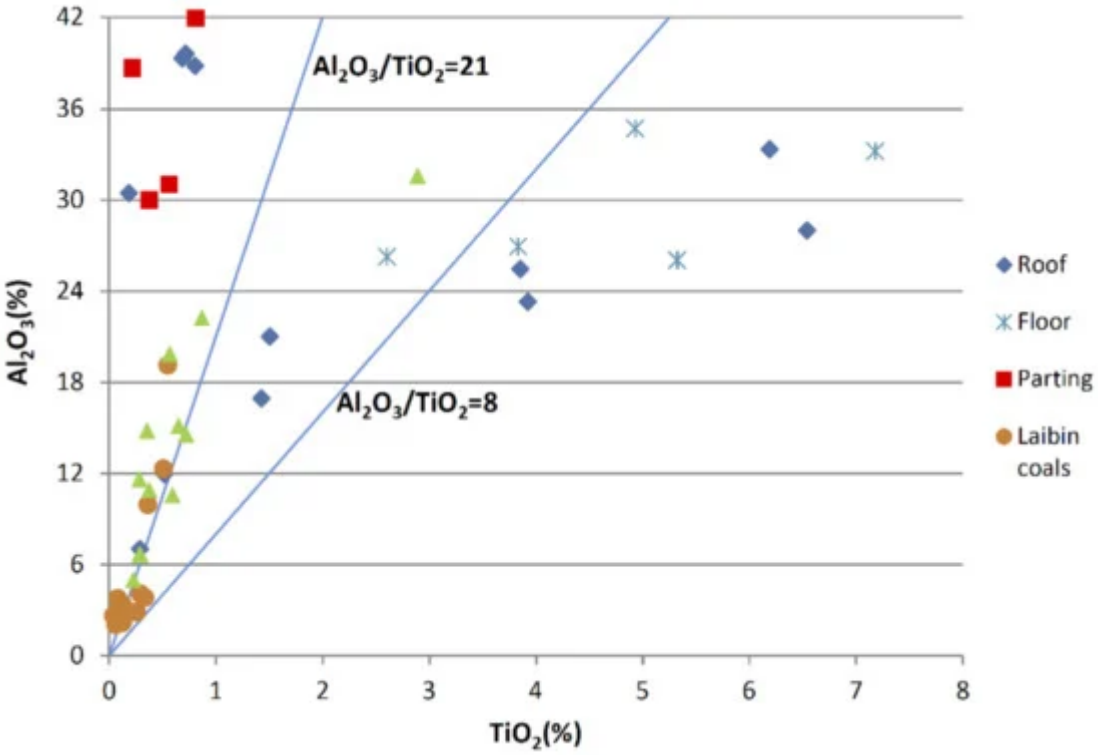

Figure 5. Plot of TiO_2 vs. Al_2O_3 for coal plies, partings, roof, and floor samples from the Bole and Laibin Mines.

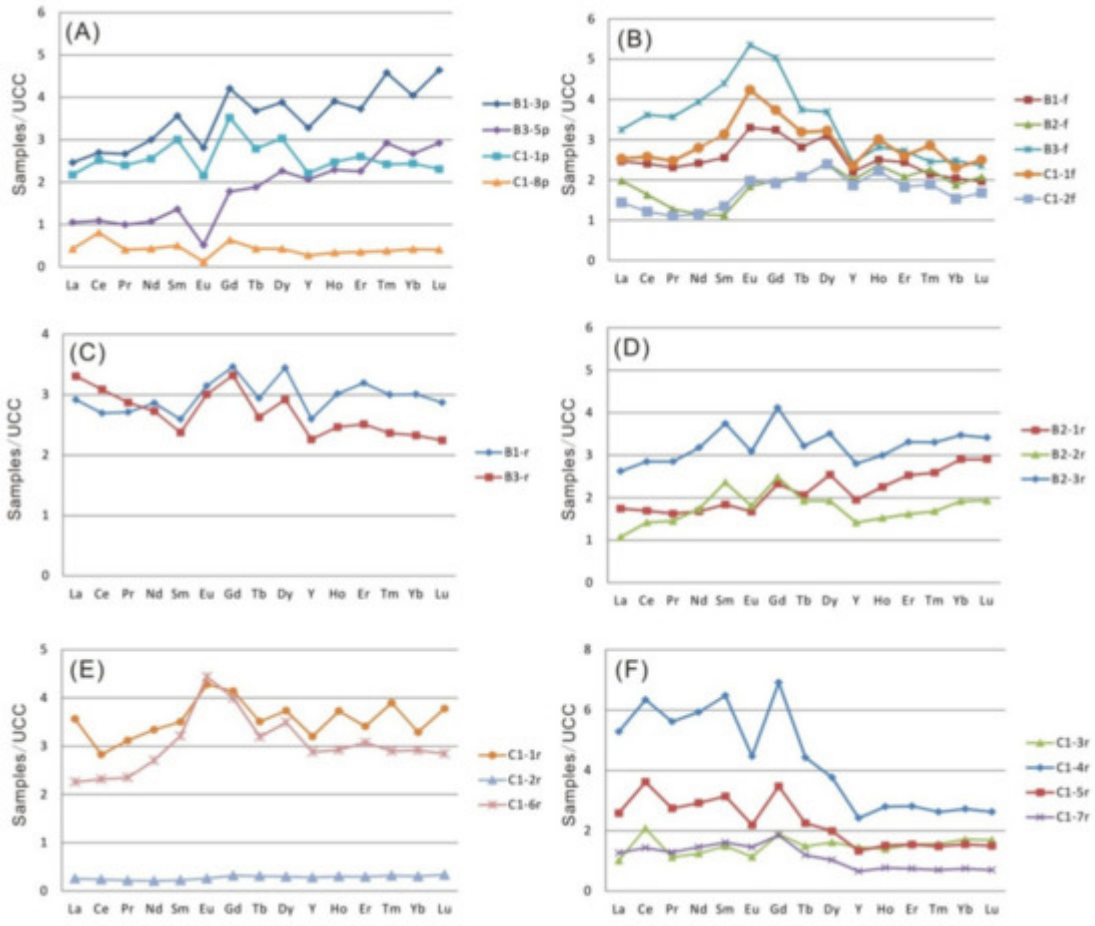

Figure 6. REY distribution patterns in the roof, floor, and parting strata of B1, B2, B3, and C1 coals. REY are normalized to an Upper Continental Crust (UCC) [55]. (**A**), parting samples in C1 Coal and B1 and B3 layers. (**B**), Floor samples of C1 Coal and B1, B2, and B3 layers. (**C**), Roof samples of B1 and B3 layers. (**D**), Roof samples of the B2 layer. (**E**,**F**), Roof samples of C1 Coal.

The floor (sample C1-2f) of the Bole mine is identified as a tuffaceous claystone derived from altered mafic volcanic ash rather than water-borne detritus from terrigenous regions, as evidenced by the cryptocrystalline kaolinite with no sedimentary layering observed (Figure 7A) and the large amount of anatase debris disseminated in the matrix (Figure 7B–F). The anatase may have been derived from volcanic ashes, as evidenced by well-developed crystals or the crystals with high-temperature cracks and embayments [21]. Meanwhile some anatase grains show the skeletal/colloidal structure, suggesting intense alteration even though anatase is usually found unaltered in mafic volcanic ash [12][20][21]. The REY enrichment pattern of sample C1-2f, characterized by M-type and H-type enrichment and weak positive Eu anomaly (Figure 6B), differs slightly from those of low-Ti basalts and are more similar to the spidergrams of high-Ti basalts (Figure 8) [56]. The enrichment of heavy REY in the sample C1-2f was likely due to the influx of hydrothermal solutions [8]. The lower Eu anomaly in sample C1-2f sample may be explained by clay alteration of feldspar, which is commonly the main carrier of Eu in magmatic rocks. A very high Ti/Y ratio (about 900) for sample C1-2f claystone indicates a high-Ti basalt as the source rock as well [56]. Such a basaltic origin is also supported by higher concentrations of Zr, Nb, V, Co, Cu, Zn, and a low Al_2O_3/TiO_2 value (4.62) for the sample.

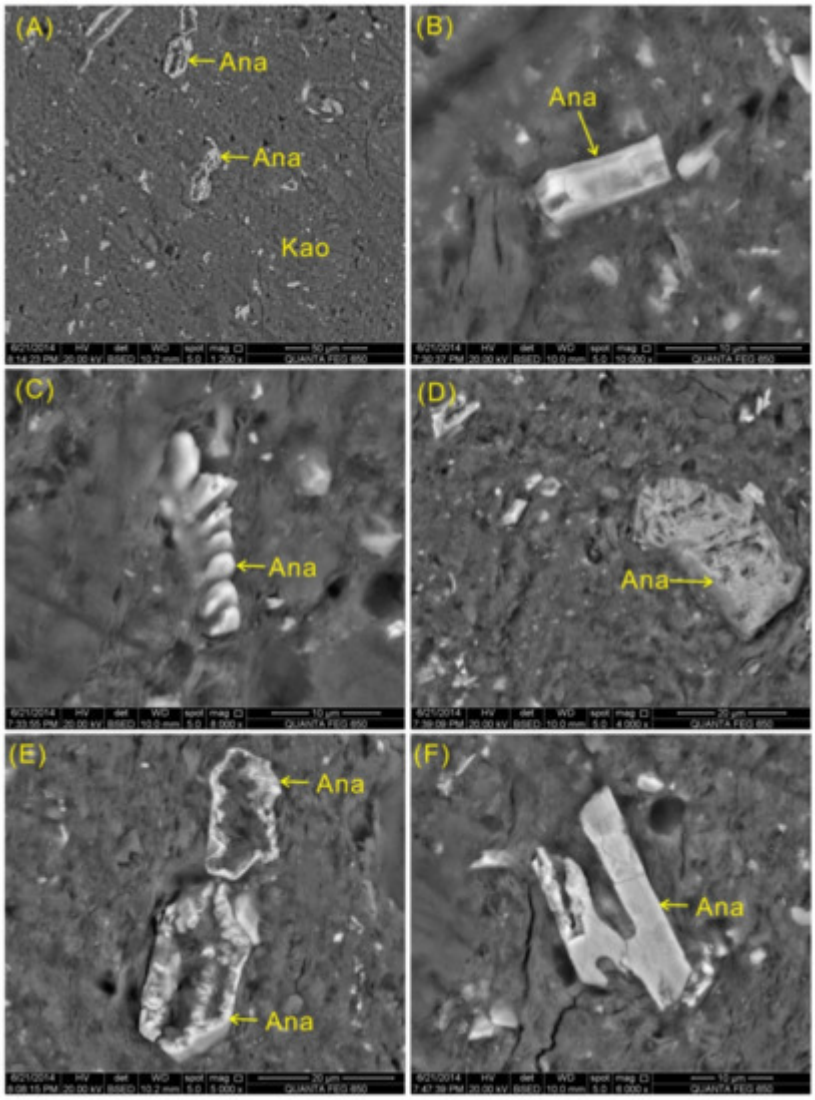

Figure 7. SEM back-scattered electron images of minerals in C1-2f. (**A**) Microcrystalline kaolinite matrix and anatase crystals. (**B**) Euhedral anatase crystal. (**C**–**E**) Altered anatase framework. (**F**) Anatase with high temperature cracks and embayments. Ana: anatase. Kao: kaolinite.

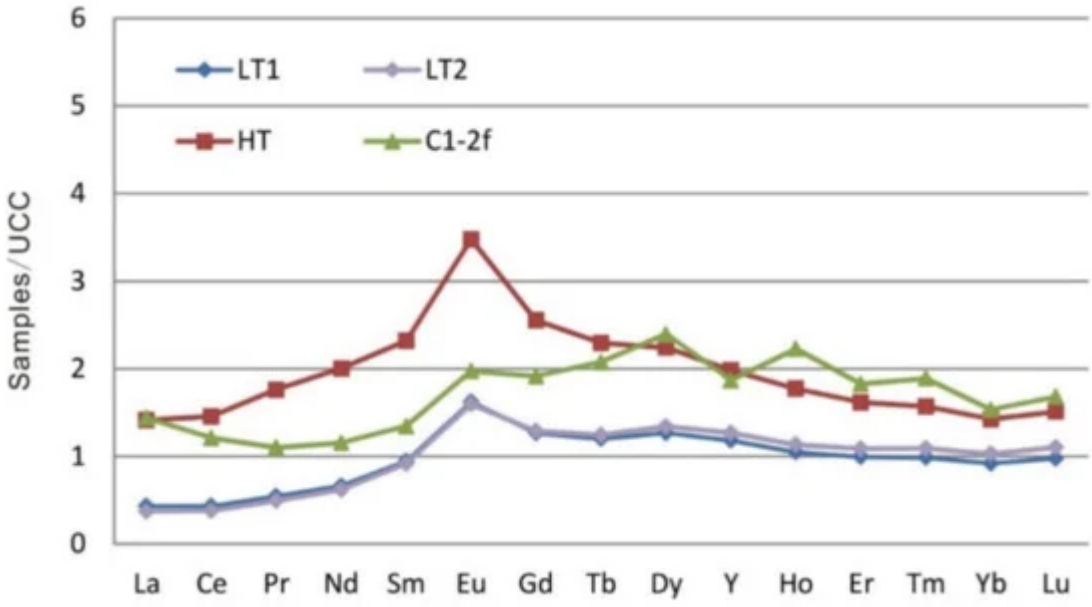

Figure 8. REY distribution patterns normalized to the Upper Continental Crust (UCC) [55] for the C1-2f sample and high-Ti and low-Ti alkali basalts of the Emeishan Province (data from Xiao et al. [56]).

The interpretation of the C1-2f claystone as tuffaceous is not contradictory with the high-Ti basalts, which were mainly erupted in the Emeishan Province some 257–260 Ma ago [57][58] because the former was deposited closer to the P-T boundary than the latter. Zhu et al. [59] found a very thick (~100 m) tuff layer from which zircons gave a laser ablation ICP-MS U-Pb age of 251 ± 1 Ma, close to the suggested depositional age for the studied rocks. These data confirm the suggestion that volcanic activity of the Emeishan Province was continuing throughout the Late Permian [48][60].

The chemical compositions in the tuffaceous floor and tonsteins present in this study are similar to those reported by Dai et al. [12][48] and Zhou et al. [22][23]. Dai et al. [48] have identified three types of tonsteins (silicic, mafic, and alkali) in the Late Permian coal seams in Southwestern China. The alkali and silicic tonsteins are mainly distributed in the early and late stages of the Late Permian, respectively. The mafic tonsteins and tuffs are distributed throughout the late Permian [48]. The three types of tonsteins have different assemblage of elevated trace elements. The mafic tonsteins and tuffs are enriched in Sc, V, Cr, Co, and Ni, and the alkali tonsteins are characterized by high contents of Nb, Ta, Zr, Hf, REY, and Ga. The silicic tonsteins contain the lowest amount of REY but have the highest fractionation between light REE and heavy REY. As suggested by Dai et al. [48], tonsteins in the Late Permian coal seams in Southwestern China may be at the periphery of the Emeishan Large Igneous Province and likely resulted from a waning activity of the plume. The three types of tonsteins were derived from different mantle sources that have been subjected to low-degree partial melting, fluid fractionation, and contamination by a lithospheric mantle [48].

2.2. Origin of Interstratified Berthierine/Chamosite

Berthierine is a common mineral in modern sediments and sedimentary rocks, and is considered to be typical of marine sediments due to the reducing environment of the seabed and the presence of abundant iron ions [31][32][33][35]. However, berthierine has also been observed in non-marine low-temperature metamorphic and hydrothermally-altered rocks [61][62][63], and in coal-bearing strata in Japan and China [20][21][64][65]. In the latter cases, berthierine may replace pre-existing minerals (e.g., kaolinite, siderite, and other Fe-rich phases) [65][66][67], directly precipitating from some Fe-bearing and Mg-bearing solutions [68][69][70] or results from the dissolution of volcanic fragments when Fe and Mg are liberated during recrystallization [21][71][72]. The coexistence of B/C with quartz or calcite (Figure 9B–E) does not necessarily indicate their genetic relations. However, the intergrowth of B/C and kaolinite (Figure 10A,B) indicates that B/C was derived from the kaolinite and Fe-rich and Mg-rich hydrothermal solutions, and that the formation mechanism of B/C is similar to that of chamosite reported by Dai et al. [29] and Wang et al. [24]. The relations between B/C and kaolinite in the floor sample (B3-f) also indicates the substitution of the former for the latter (Figure 11C,D).

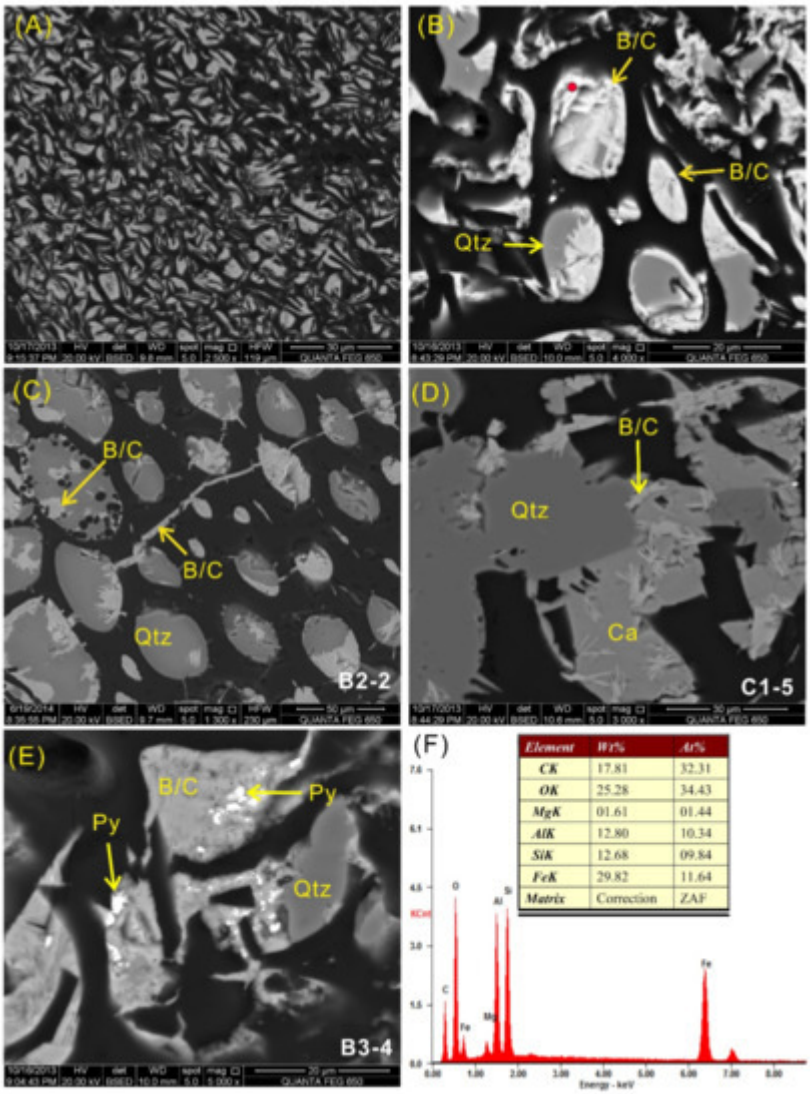

Figure 9. SEM back-scattered electron images of cell-filling minerals in coal samples and EDS data of a selected point. (**A**) Interstratified berthierine/chamosite as cell-infillings in sample C1-5. (**B**) Quartz coated with interstratified berthierine/chamosite as cell-infillings in sample B3-4. (**C**–**E**) Cell-filing interstratified berthierine/chamosite, quartz,

calcite, and pyrite in samples B2-2 (**C**), sample C1-5 (**D**), and B3-4 (**E**). (**F**) EDS spectrum of point 1 in (**B**). Qtz: quartz. B/C: interstratified berthierine/chamosite. Py: pyrite. Ca: calcite.

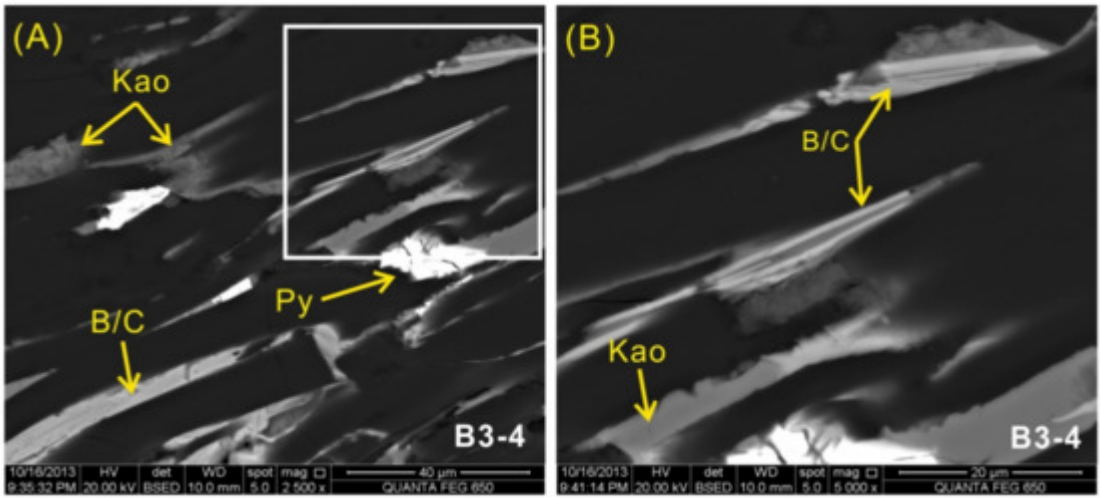

Figure 10. SEM back-scattered electron images of clay minerals in coal sample B3-4. (**A**) Cell-filling interstratified berthierine/chamosite, kaolinite, and pyrite. (**B**) Enlargement of rectangle in (**A**). B/C: interstratified berthierine/chamosite. Kao: kaolinite. Py: pyrite.

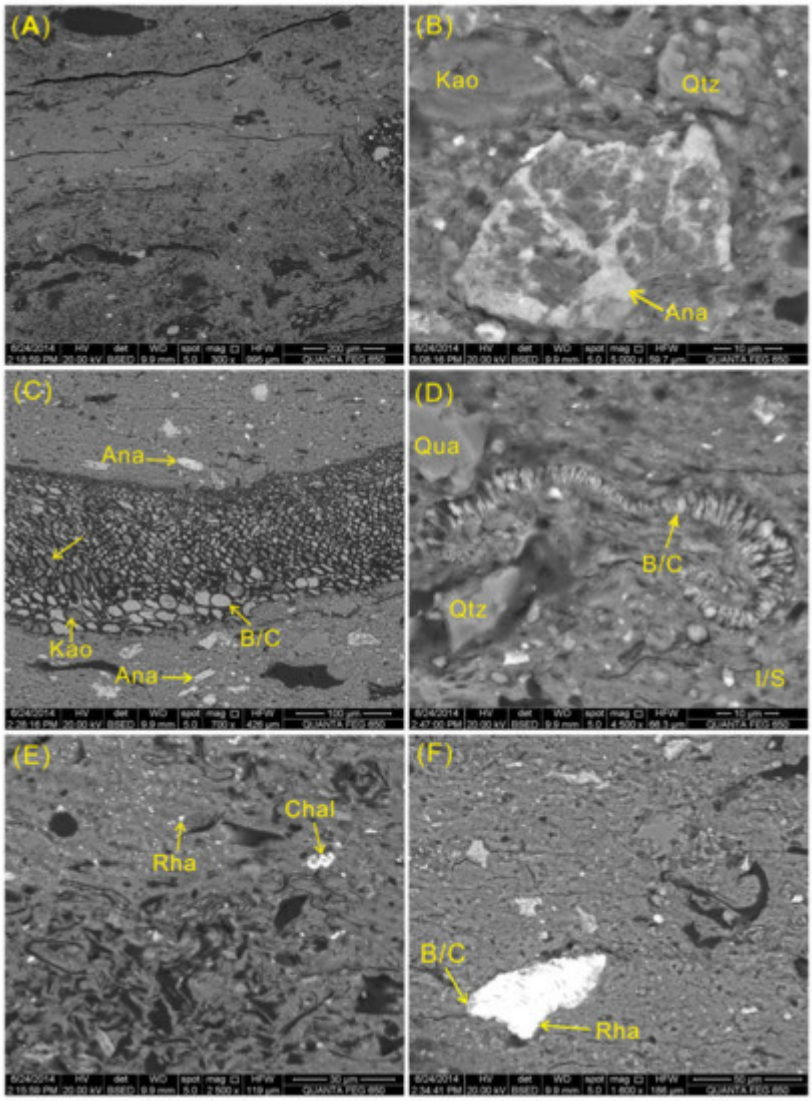

Figure 11. SEM back-scattered electron images of minerals in B3-f. (**A**) Clay minerals as matrix with abundant plant residues. (**B**) Kaolinite, authigenic quartz, and highly altered anatase with network texture. (**C**) Cell-filling kaolinite and B/C. (**D**) Vermicular B/C and authigenic quartz. (**E**) Small grains (<1 μm) of rhabdophane. (**F**) Rhabdophane and associated B/C. B/C: interstratified berthierine/chamosite. Kao: kaolinite. Qtz: quartz. Ana: anatase. I/S: mixed layer illite/smectite. Chal: chalcopyrite. Rha: rhabdophane.

Berthierine is generally considered relatively stable in low-temperature (<200 °C) reduced environments [69][63][64][67][73]. As the temperature increases, it can be transformed into chamosite or occur as an interstratification phase in a certain temperature range. Iijima and Matsumoto [64] proposed that the formation temperature of berthierine in the Paleogene and Late Triassic coals of Japan is 65–150 °C, and its transformation to chamosite occurred at 160 °C. A similar crystallization temperature for berthierine (150 °C) was also reported by Rivas-Sanchez et al. [73]. Based on the ratio of mixed layer I/S and the occurrence of berthierine, Zhao et al. [74] inferred that the diagenesis temperature of polymetallic mineralized beds in Eastern Yunnan is 100–160 °C, sometimes reaching 180 °C. Ryan and Hillier [69] showed that interstratified berthierine/chamosite was stable in the range of temperatures between 90 and 200 °C in Late Jurassic sandstones, U.S. Gulf Coast. Therefore, the formation of B/C in the samples investigated in this study was most likely under a low-temperature regime (i.e., <200 °C).

Moreover, the REE-phosphates (rhabdophane and florencite) observed in the coals and non-coal samples of the present study (Figure 12C,D, and Figure 11F) may also be related to low-temperature solutions [75][76][77]. It should be mentioned, however, that the suggested temperature of authigenic mineralization corresponds to both ascending-hydrothermal and heated-meteoric solutions, for which the transitional field is between 25–50 °C and 200 °C [78]. Therefore, this study does not answer the question regarding the sources of the studied authigenic mineralization regarding whether they were from a deeper source or related to weathering and other near-surface processes. It is most likely that both deep and near-surface processes have complexly influenced the Late Permian coal basins of SW China, as suggested by Dai et al. [79].

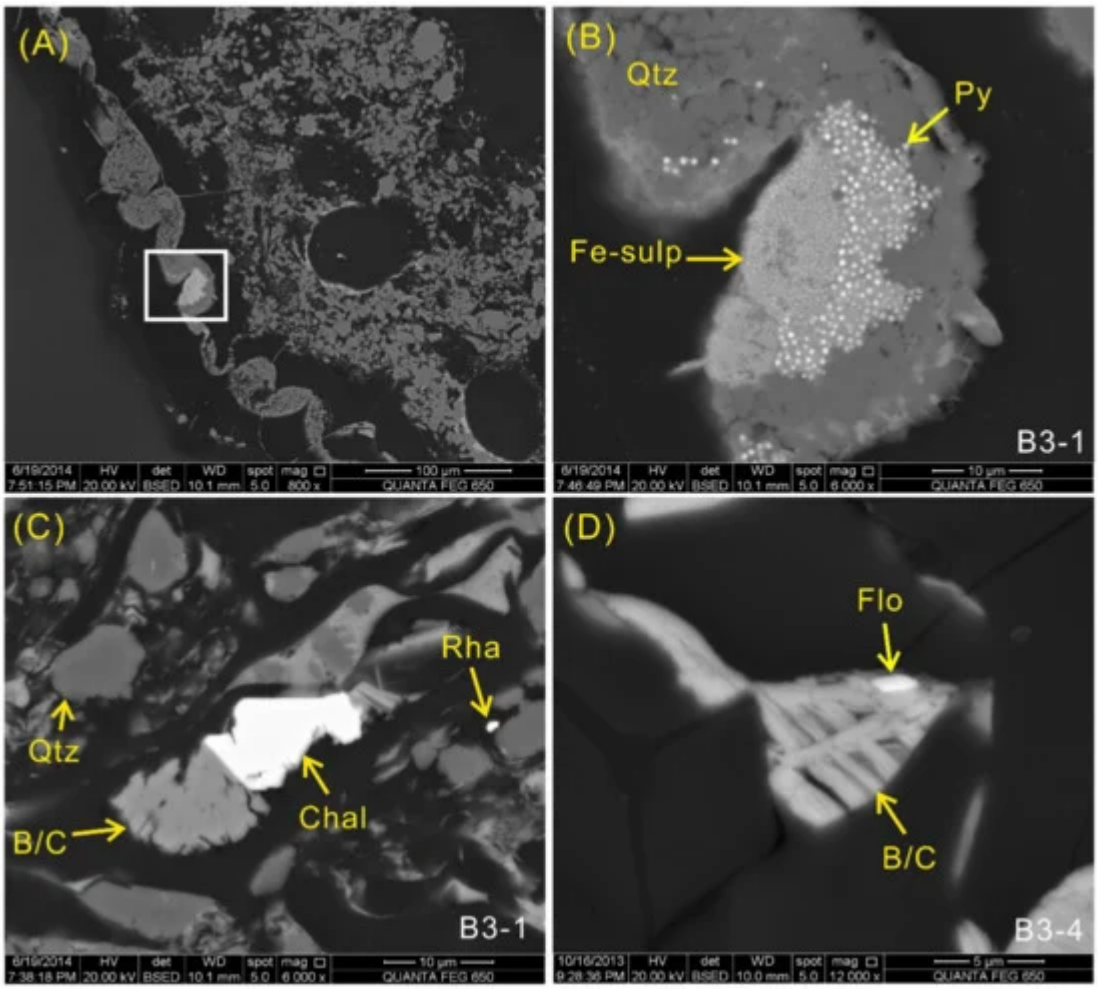

Figure 12. SEM back-scattered electron images of minerals in coal samples. (**A**) Cell-filling pyrite, iron-sulphate mineral, and quartz in sample B3-1. (**B**) Enlargement of rectangle in (**A**). (**C**) Rhabdophane and cell-filling chalcopyrite, quartz, and interstratified berthierine/chamosite in sample B3-1. (**D**) Cell-filling florencite and interstratified berthierine/chamosite in sample B3-4. B/C: interstratified berthierine/chamosite. Qtz: quartz. Py: pyrite. Fe-sulp: Fe-sulfate mineral. Rha: rhabdophane. Chal: chalcopyrite. Flo: florencite. B/C: interstratified berthierine/chamosite.

2.3. Origin of Quartz and Other Minerals

Quartz of authigenic origin is common in the Late Permian coals of Southwestern China, especially Eastern Yunnan Province. It is considered that the quartz was derived from silica-containing solutions originating from the weathering of volcanic rocks in the Kangdian Upland or from post-depositional silica-rich fluids [12][29]. The occurrence modes of quartz (Figure 13) in the studied coal samples indicates that the silica-rich fluid input was either from the sediment-source region or from fluid sources during peat accumulation or before peat compaction. The authigenic quartz in the samples may also be derived from desilicification of the volcanic ashes. Soluble Si from the volcanic ashes may then have re-precipitated in the pores of the underlying peat [1][80]. Desilicification of the volcanic ashes in the peat swamp has been commonly observed in many coalfields [10][18]. However, it is not necessary for hydrothermal solutions to take part in the desilicification process as the process can occur during the syngentic (peat deposition) or diagentic (rank advance) stages.

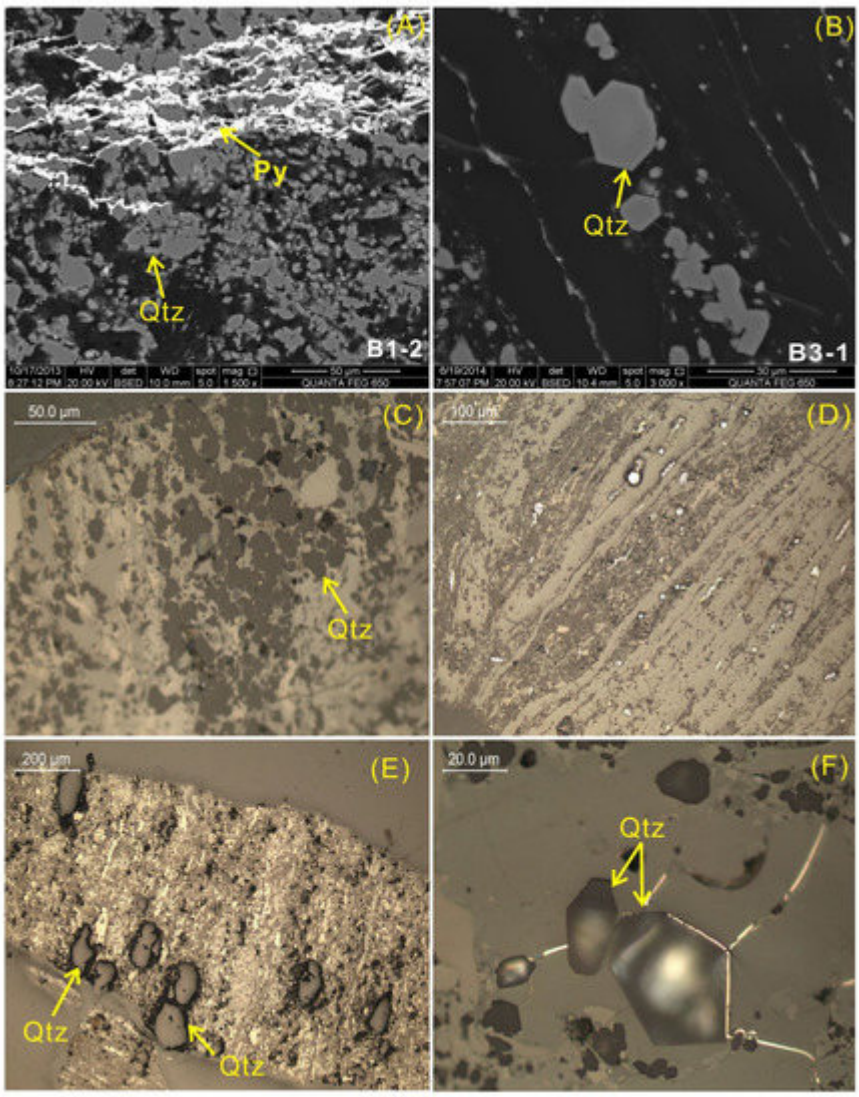

Figure 13. Quartz in the coal samples. (**A**) Authigenic quartz and fracture-filling pyrite in sample B1-2. (**B**,**C**) Fine-grained quartz in collodetrinite in sample B3-1. (**D**) Small quartz particles and framboidal pyrite along the lamination planes in sample B1-1**.** (**E**) Detrital quartz in sample B2-1. (**F**) Hexagonal bipyramid quartz rimmed by epigenetic pyrite in sample B3-1. (**A**,**B**), Back-scattered electron images. (**C**–**F**), Optical microscope, reflected light in air. Qtz: quartz. Py: pyrite.

The modes of occurrence of framboidal pyrite within collodetrinite (Figure 13) show that the mineral was formed at syngenetic and/or early diagenetic stages during or shortly after the peat accumulation. Other authigenic minerals, including fracture-filling pyrite (or iron-sulphate minerals) and calcite (Figure 13 and Figure 4), euhedral gypsum in the tonstein (B3-5p) (Figure 4) and rhabdophane in the floor sample (B3-f) (Figure 11) suggest epigenetic deposition.

3. Conclusions

The coals from the No. C1 (B1, B2, and B3) coal seam of the Bole and Laibin mines, Eastern Yunnan, are mainly medium-high ash, low-sulphur bituminous coal. The minerals in the coals are mainly dominated by quartz and interstratified berthierine/chamosite, along with varying proportions of kaolinite, mixed layer I/S, calcite, anatase, pyrite, bassanite, chalcopyrite, and REE-phosphates. Low-temperature solutions are a very important factor responsible for the mineralogical compositions during the diagenetic process. Abundant authigenic quartz is the result of silica-rich solution inputs during peat accumulation or before peat compaction. The coexisting calcite as cell-infillings may have been leached from the Maokou limestones. Interstratified berthierine/chamosite in the coals is largely formed from direct precipitation of Fe-Mg-rich hydrothermal fluids, likely after the formation of quartz. However, berthierine (B/C) in the floor strata were derived from the interaction of kaolinite with the hydrothermal fluids. In addition, minor minerals including pyrite, anatase, REE-phosphates, chalcopyrite, and gypsum are also derived from multi-stage hydrothermal fluids as indicated by the presence of berthierine (B/C) and REE-phosphates. The diagenetic environment for the formation of the coal seams is suggested to be of a low temperature (<200 °C).

The multi-stage volcanic ash deposition plays another key role in coal formation. Four thin intra-seam claystones (partings) within the coal seams are identified as tonstein layers, mainly evidenced by cryptocrystalline and vermicular kaolinite, along with minor proportions of high-temperature quartz, volcanic zircon, apatite, monazite, and anatase. The tonsteins are likely derived from felsic volcanic ash, which are characterized by high Al_2O_3/TiO_2 values (51.6–179) and negative Eu anomalies.

Based on the modes of occurrence of its minerals, higher concentrations of Zr, Nb, V, Co, Cu, Zn, low Al_2O_3/TiO_2 (4.62), and high Ti/Y value, as well as the M-type distribution pattern of rare earth elements and the positive Eu anomaly, the floor sample of the Bole mine (C1-2f) is identified as a tuffaceous claystone consisting of altered mafic volcanic (high-Ti basalt of the Emeishan large igneous province) rather than detrital materials from sediment source regions.

References

1. Ward, C.R. Analysis and significance of mineral matter in coal seams. Int. J. Coal Geol. 2002, 50, 135–168.

2. Ward, C.R. Analysis, origin and significance of mineral matter in coal: An updated review. Int. J. Coal Geol. 2016, 165, 1–27.
3. Finkelman, R.B.; Dai, S.; French, D. The importance of minerals in coal as the hosts of chemical elements. Int. J. Coal Geol. 2019, 212, 103251.
4. Ren, D. Mineral matters in coal. In Coal Petrology of China; Han, D.X., Ed.; Publishing House of China University of Mining and Technology: Xuzhou, China, 1996; pp. 67–77. (In Chinese)
5. Dai, S.; Ren, D.; Chou, C.L.; Finkelman, R.B.; Seredin, V.V.; Zhou, Y. Geochemistry of trace elements in Chinese coals: A review of abundances, genetic types, impacts on human health, and industrial utilization. Int. J. Coal Geol. 2012, 94, 3–21.
6. Huang, X.; Gordon, T.; Rom, W.N.; Finkelman, R.B. Interaction of iron and calcium minerals in coals and their roles in coal dust-induced health and environmental problems. Rev. Miner. Geochem. 2006, 64, 153–178.
7. Seredin, V.V. From coal science to metal production and environmental protection: A new story of success. Int. J. Coal Geol. 2012, 90–91, 1–3.
8. Seredin, V.V.; Dai, S. Coal deposits as potential alternative sources for lanthanides and yttrium. Int. J. Coal Geol. 2012, 94, 67–93.
9. Dai, S.; Yan, X.; Ward, C.R.; Hower, J.C.; Zhao, L.; Wang, X.; Zhao, L.; Ren, D.; Finkelman, R.B. Valuable elements In Chinese coals: A review. Int. Geol. Rev. 2018, 60, 590–620.
10. Dai, S.; Ward, C.R.; Graham, I.T.; French, D.; Hower, J.C.; Zhao, L.; Wang, X. Altered volcanic ashes in coal and coal-bearing sequences: A review of their nature and significance. Earth Sci. Rev. 2017, 175, 44–74.
11. Ren, D.; Zhao, F.; Dai, S.; Zhang, J.; Luo, K. Geochemistry of Trace Elements in Coal; Science Press: Beijing, China, 2006; p. 556. (In Chinese)
12. Dai, S.; Li, T.; Seredin, V.V.; Ward, C.R.; Hower, J.C.; Zhou, Y.; Zhang, M.; Song, X.; Song, W.; Zhao, C. Origin of minerals and elements in the Late Permian coals, tonsteins, and host rocks of the Xinde Mine, Xuanwei, eastern Yunnan, China. Int. J. Coal Geol. 2014, 121, 53–78.
13. Dai, S.; Liu, J.; Ward, C.R.; Hower, J.C.; French, D.; Jia, S.; Hood, M.M.; Garrison, T.M. Mineralogical and geochemical compositions of late Permian coals and host rocks from the Guxu coalfield, Sichuan province, China, with emphasis on enrichment of rare metals. Int. J. Coal Geol. 2016, 166, 71–95.
14. Raymond, R.; Andrejeko, M.J. Mineral. Matter in Peat: Its Occurrence, Form, and Distribution; Report LA9907 OBES; Los Alamos National Laboratory: Los Alamos, NM, USA, 1983; p. 242.
15. Cobb, J.C. Timing and development of mineralized veins during diagenesis in coal beds. In Proceedings of the 9th International Congress on Carboniferous Stratigraphy and Geology,

Urbana, IL, USA, 19 May 1979; Cross, A.T., Ed.; Southern Illinois University Press: Carbondale, IL, USA, 1985; Volume 4, pp. 371–376.

16. Burger, K.; Zhou, Y.; Tang, D. Synsedimentary volcanic ash derived illitic tonsteins in Late Permian coal-bearing formations of southwestern China. Int. J. Coal Geol. 1990, 15, 341–356.
17. Bohor, B.F.; Triplehorn, D.M. Tonsteins: Altered Volcanic-Ash Layers in Coal-Bearing Sequences; Special Paper 285; Geological Society of America: Boulder, CO, USA, 1993; p. 44.
18. Spears, D.A. The origin of tonsteins, an overview, and links with seatearths, fireclays and fragmental clay rocks. Int. J. Coal Geol. 2012, 94, 22–31.
19. Dai, S.; Guo, W.; Nechaev, V.P.; French, D.; Ward, C.R.; Spiro, B.F.; Finkelman, R.B. Modes of occurrence and origin of mineral matter in the Palaeogene coal (No. 19-2) from the Hunchun Coalfield, Jilin Province, China. Int. J. Coal Geol. 2018, 189, 94–110.
20. Zhao, L.; Dai, S.; Graham, I.T.; Li, X.; Zhang, B. New insights into the lowest Xuanwei Formation in eastern Yunnan Province, SW China: Implications for Emeishan large igneous province felsic tuff deposition and the cause of the end-Guadalupian mass extinction. Lithos 2016, 264, 375–391.
21. Zhao, L.; Dai, S.; Graham, I.T.; Li, X.; Liu, H.; Song, X.; Hower, J.C.; Zhou, Y. Cryptic sediment-hosted critical element mineralization from eastern Yunnan Province, southwestern China: Mineralogy, geochemistry, relationship to Emeishan alkaline magmatism and possible origin. Ore Geol. Rev. 2017, 80, 116–140.
22. Zhou, Y.; Ren, Y.; Bohor, B.F. Origin and distribution of tonsteins in Late Permian coal seams of southwestern China. Int. J. Coal Geol. 1982, 2, 49–77.
23. Zhou, Y.; Bohor, B.F.; Ren, Y. Trace element geochemistry of altered volcanic ash layers (tonsteins) in Late Permian coal-bearing formations of eastern Yunnan and western Guizhou Province, China. Int. J. Coal Geol. 2000, 44, 305–324.
24. Wang, X.; Dai, S.; Chou, C.-L.; Zhang, M.; Wang, J.; Song, X.; Wang, W.; Jiang, Y.; Zhou, Y.; Ren, D. Mineralogy and geochemistry of Late Permian coals from the Taoshuping Mine, Yunnan Province, China: Evidences for the sources of minerals. Int. J. Coal Geol. 2012, 96, 49–59.
25. Wang, X.; Zhang, M.; Zhang, W.; Wang, J.; Zhou, Y.; Song, X.; Li, T.; Li, X.; Liu, H.; Zhao, L. Occurrence and origins of minerals in mixed-layer illite/smectite-rich coals of the Late Permian age from the Changxing Mine, eastern Yunnan, China. Int. J. Coal Geol. 2012, 102, 26–34.
26. Large, D.J.; Kelly, S.; Spiro, B.; Tian, L.; Shao, L.; Finkelman, R.; Zhang, M.; Somerfield, C.; Plint, S.; Ali, Y.; et al. Silica-volatile interaction and the geological cause of the Xuan Wei lung cancer epidemic. Environ. Sci. Technol. 2009, 43, 9016–9021. [PubMed]

27. Tian, L. Coal Combustion Emissions and Lung Cancer in Xuan Wei, China. Ph.D. Thesis, University of California, Berkeley, CA, USA, 2005.
28. Li, J. Fe-Rich Chamosite in Coal and Lung Cancer in Xuan Wei, China. Ph.D. Thesis, University of Hong Kong, Pokfulam, Hong Kong, China, 2019.
29. Dai, S.; Tian, L.; Chou, C.-L.; Zhou, Y.; Zhang, M.; Zhao, L.; Wang, J.; Yang, Z.; Cao, H.; Ren, D. Mineralogical and compositional characteristics of Late Permian coals from an area of high lung cancer rate in XuanWei, Yunnan, China: Occurrence and origin of quartz and chamosite. Int. J. Coal Geol. 2008, 76, 318–327.
30. Dai, S.; Chou, C.-L. Occurrence and origin of minerals in a chamosite-bearing coal of Late Permian age, Zhaotong, Yunnan, China. Am. Miner. 2007, 92, 1253–1261.
31. Bhattacharyya, D.P. Origin of berthierine in ironstones. Clay Clay Min. 1983, 31, 173–182.
32. Van Houten, F.B.; Purucker, M.E. Glauconitic peloids and chamositic ooids—Favorable factors, constraints, and problems. Earth Sci. Rev. 1984, 20, 211–243.
33. Macquaker, J.H.S.; Taylor, K.G.; Young, T.P.; Curtis, C.D. Sedimentological and geochemical controls on ooidal ironstone and ‘bone-bed’ formation and some comments on their sequence stratigraphic significance. In Sequence Stratigraphy in British Geology; Hesselbo, S., Parkinson, D.N., Eds.; Geological Society of London Special Publication: London, UK, 1996; Volume 103, pp. 97–107.
34. Boyd, G.A.; Wallace, M.W.; Holdgate, G.R.; Gallagher, S.J. Marine clays and porosity evolution in the Nullawarre Greensand, Otway Basin, southeastern Australia. Pet. Explor. Soc. Aust. 2004, II, 1–16.
35. Huggett, J.M.; Gale, A.S.; McCarty, D. Petrology and palaeoenvironmental significance of authigenic iron-rich clays, carbonates and apatite in the Claiborne Group, Middle Eocene, NE Texas. Sediment. Geol. 2010, 228, 119–139.
36. Lyons, P.C.; Spears, D.A.; Outerbridge, W.F.; Congdon, R.D.; Evans, H.T. Euramerican tonsteins: Overview, magmatic origin, and depositional-tectonic implications. Palaeogeogr. Palaeoclim. Palaeoecol. 1994, 106, 113–134.
37. Zhou, Y.; Burger, K.; Tang, D. A new development of research on the tonsteins (clay rock partings) in Late Permian coal measures, Southwest China. Yunnan Geol. 1988, 7, 213–228, (In Chinese with English abstract).
38. Zhou, Y.; Ren, Y. Origin and geological significance of tonsteins in the Late Permian coals from eastern Yunnan, China. Yunnan Geol. 1983, 2, 38–46, (In Chinese with English abstract).
39. Zhao, L.; Ward, C.R.; French, D.; Graham, I.T. Mineralogical composition of Late Permian coal seams in the Songzao Coalfield, southwestern China. Int. J. Coal Geol. 2013, 116–117, 208–226.

40. Ruppert, L.F.; Moore, T.A. Differentiation of volcanic ash-fall and water-borne detrital layers in the Eocene Senakin coal bed, Tanjung Formation, Indonesia. Org. Geochem. 1993, 20, 233–247.
41. Spears, D.A. The mineralogy of the Stafford tonstein. P. Yorks. Geol. Soc. 1971, 38, 497–516.
42. Zhao, L.; Ward, C.R.; French, D.; Graham, I.T. Mineralogy of the volcanic influenced Great Northern coal seam in the Sydney Basin, Australia. Int. J. Coal Geol. 2012, 94, 94–110.
43. Spears, D.A.; Kanaris-Sotiriou, R. A geochemical and mineralogical investigation of some British and other European tonsteins. Sedimentology 1979, 26, 407–425.
44. Triplehorn, D.M.; Stanton, R.W.; Ruppert, L.F.; Crowley, S.S. Volcanic ash dispersed in the Wyodak–Anderson coal bed, Powder River Basin, Wyoming. Org. Geochem. 1991, 17, 567–575.
45. Hower, J.C.; Ruppert, L.F.; Eble, C.F. Lanthanide, yttrium, and zirconium anomalies in the fire clay coal bed, eastern Kentucky. Int. J. Coal Geol. 1999, 39, 141–153.
46. Zhou, Y.; Ren, Y.; Tang, D.; Bohor, B. Characteristics of zircons from volcanic ash derived tonsteins in Late Permian coal fields of eastern Yunnan, China. Int. J. Coal Geol. 1994, 25, 243–264.
47. He, B.; Xu, Y.; Wang, Y.; Luo, Z. Sedimentation and lithofacies paleogeography in Southwestern China before and after the Emeishan flood volcanism: New Insights into surface response to mantle plume activity. J. Geol. 2006, 114, 17–132.
48. Liu, J.; Nechaev, V.P.; Dai, S.; Song, H.; Nechaeva, E.V.; Jiang, Y.; Graham, I.T.; French, D.; Yang, P.; Hower, J.C. Evidence for multiple sources for inorganic components in the Tucheng coal deposit, western Guizhou, China and the lack of critical-elements. Int. J. Coal Geol. 2020, 223, 103468.
49. Finlow-Bates, T.; Stumpfl, E.F. The behaviour of so-called immobile elements in hydrothermally altered rocks associated with volcanogenic submarine-exhalative ore deposits. Min. Depos. 1981, 16, 319–328.
50. Zhou, Y. The synsedimentary alkalinity-volcanic ash derived tonsteins of Early Longtan age in south-western China. Coal Geol. Explor. 1999, 27, 5–9, (In Chinese with English abstract).
51. Hayashi, K.-I.; Fujisawa, H.; Holland, H.D.; Ohmoto, H. Geochemistry of ~1.9 Ga sedimentary rocks from northeastern Labrador, Canada. Geochim. Cosmochim. Acta 1997, 61, 4115–4137.
52. Isozaki, Y.; Yao, J.; Matsuda, T.; Sakai, H.; Ji, Z.; Shimizu, N.; Kobayashi, N.; Kawahata, H.; Nishi, H.; Takano, M.; et al. Stratigraphy of the Middle-Upper Permian and Lowermost Triassic at Chaotian, Sichuan, China Record of Late Permian double mass extinction event. Proc. Jpn. Acad. B 2004, 80, 10–16.
53. He, B.; Zhong, Y.; Xu, Y.; Li, X. Triggers of Permo-Triassic boundary mass extinction in South China: The Siberian Traps or Paleo-Tethys ignimbrite flare-up? Lithos 2014, 204, 258–267.

54. Liao, Z.; Hu, W.; Cao, J.; Wang, X.; Yao, S.; Wu, H.; Wan, Y. Heterogeneous volcanism across the Permian–Triassic Boundary in South China and implications for the Latest Permian Mass Extinction: New evidence from volcanic ash layers in the Lower Yangtze Region. J. Asian Earth Sci. 2016, 127, 197–210.
55. Taylor, S.R.; McLennan, S.M. The Continental Crust: Its Composition and Evolution; Blackwell: Oxford, UK, 1985; p. 312.
56. Xiao, L.; Xu, Y.; Mei, H.; Zheng, Y.; He, B.; Pirajno, F. Distinct mantle sources of low-Ti and high-Ti basalts from the western Emeishan large igneous province, SW China: Implications for plume–lithosphere interaction. Earth Planet. Sci. Lett. 2004, 228, 525–546.
57. Xu, Y.; Chung, S.; Shao, H.; He, B. Silicic magmas from the Emeishan large igneous province, Southwest China: Petrogenesis and their link with the end-Guadalupian biological crisis. Lithos 2010, 119, 47–60.
58. Li, Y.; He, H.; Ivanov, A.V.; Demonterova, E.I.; Pan, Y.; Deng, C.; Zheng, D.; Zhu, R. 40Ar/39Ar age of the onset of high-Ti phase of the Emeishan volcanism strengthens the link with the end-Guadalupian mass extinction. Int. Geol. Rev. 2018, 60, 1906–1917.
59. Zhu, J.; Zhang, Z.; Hou, T.; Kang, J. LA-ICP-MS zircon U-Pb geochronology of the tuffs on the uppermost of the Emeishan basalt succession in Panxian County, Guizhou Province: Constraints on genetic link between Emeishan large igneous province and the mass extinction. Acta Pet. Sin. 2011, 27, 2743–2751, (In Chinese with English abstract).
60. Dai, S.; Chekryzhov, I.Y.; Seredin, V.V.; Nechaev, V.P.; Graham, I.T.; Hower, J.C.; Ward, C.R.; Ren, D.; Wang, X. Metalliferous coal deposits in East Asia (Primorye of Russia and South China): A review of geodynamic controls and styles of mineralization. Gondwana Res. 2016, 29, 60–82.
61. Jiang, W.; Peacor, D.R.; Okita, P.M. Hydrothermal and metamorphic berthierine from the Kidd Creek volcanogenic massive sulfide deposit, Timmins, Ontario. Can. Miner. 1992, 30, 1127–1142.
62. Taylor, K.G. Berthierine from the non-marine Wealden (Early Cretaceous) sediments of South-East England. Clay Min. 1990, 25, 391–399.
63. Hornibrook, E.R.C.; Longstaffe, F.J. Berthierine from the lower cretaceous Clearwater formation, Alberta, Canada. Clays Clay Min. 1996, 44, 1–21.
64. Iijima, A.; Matsumoto, R. Berthierine and chamosite in coal measures of Japan. Clays Clay Min. 1982, 30, 264–274.
65. Liu, Q.; Zhang, P. The Composition and Mineralization Mechanism of Kaolinite Rocks in Late-Palaeozoic Coal Measures, North China; China Ocean Press: Beijing, China, 1997; pp. 43–46. (In Chinese)

66. Burton, J.H.; Krinsley, D.H.; Pye, K. Authigenesis of kaolinite and chlorite in Texas Gulf Coast sediments. Clays Clay Min. 1987, 35, 291–296.
67. Rivard, C.; Pelletier, M.; Michau, N.; Razafitianamaharavo, A.; Bihannic, I.; Abdelmoula, M.; Ghanbaja, J.; Villiéras, F. Berthierine-like mineral formation and stability during the interaction of kaolinite with metallic iron at 90 °C under anoxic and oxic conditions. Am. Miner. 2013, 98, 163–180.
68. Hillier, S.; Velde, B. Chlorite interstratified with a 7A mineral: An example from offshore Norway and possible implications for the interpretation of the composition of diagenetic chlorites. Clay Min. 1992, 27, 475–486.
69. Ryan, P.C.; Reynolds, R.C. The origin and diagenesis of grain-coating serpentine-chlorite in Tuscaloosa Formation sandstone, U.S. Gulf Coast. Am. Miner. 1996, 81, 213–225.
70. Humprheys, B.A.; Smith, S.A.; Strong, G.E. Authigenic chlorite formation in late Triassic sandstones from the Central Graben, North Sea. Clay Min. 1989, 24, 427–444.
71. Boles, J.R.; Franks, S.G. Clay diagenesis in Wilcox sandstones of southwest Texas: Implications of smectite diagenesis on sandstone cementation. J. Sediment. Pet. 1979, 49, 55–70.
72. Hower, J.C.; Eslinger, E.V.; Hower, M.E.; Perry, E.A. Mechanism of burial metamorphism of argillaceous sediments. Geol. Soc. Am. Bull. 1976, 87, 125–737.
73. Rivas-sanchez, M.L.; Alva-valdivia, L.M.; Arenas-alatorre, J.; Urrutia-Fucugauchi, J.; Ruiz-Sandoval, M.; Ramos-Molina, M.A. Berthierine and chamosite hydrothermal: Genetic guides in the Peña Colorada magnetite-bearing ore deposit, Mexico. Earth Planets Space 2006, 58, 1389–1400.
74. Zhao, L.; Dai, S.; Graham, I.T.; Wang, P. Clay mineralogy of coal-hosted Nb-Zr-REE-Ga mineralized beds from Late Permian Strata, Eastern Yunnan, SW China: Implications for paleotemperature and origin of the micro-quartz. Minerals 2016, 6, 45.
75. Nriagu, J.O.; Moore, P.B. Phosphate Minerals; Springer: Berlin, Germany, 1984.
76. Smith, M.; Henderson, P.; Campbell, L. Fractionation of the REE during hydrothermal processes: Constraints from the Bayan Obo Fe-REE-Nb deposit, Inner Mongolia, China. Geochim. Cosmochim. Acta 2000, 64, 3141–3160.
77. Berger, A.; Gnos, E.; Janots, E.; Fernandez, A.; Giese, J. Formation and composition of rhabdophane, bastnäsite and hydrated thorium minerals during alteration: Implications for geochronology and low-temperature processes. Chem. Geol. 2008, 254, 238–248.
78. Guilbert, J.M.; Park, C.F., Jr. The Geology of Ore Deposits, 4th ed.; W.H. Freeman: New York, NY, USA, 1986; p. 985.

79. Dai, S.; Nechaev, V.P.; Chekryzhov, I.Y.; Zhao, L.; Vysotskiy, S.V.; Graham, I.; Ward, C.R.; Ignatiev, A.V.; Velivetskaya, T.A.; Zhao, L.; et al. A model for Nb–Zr–REE–Ga enrichment in Lopingian altered alkaline volcanic ashes: Key evidence of H-O isotopes. Lithos 2018, 302–303, 359–369.
80. Ward, C.R.; Crouch, A.; Cohen, D.R. Identification of frictional ignition potential for rocks in Australian coal mines. In Safety in Mines: The Role of Geology; Doyle, R., Moloney, J., Rogis, J., Sheldon, M., Eds.; Coalfield Geology Council of New South Wales: Maitland NSW, Australia, 1997; pp. 169–175.

Retrieved from https://encyclopedia.pub/entry/history/show/15517